Acta Geodyn. Geomater., Vol. 14, No. 3 (187), 341–355, 2017
DOI: 10.13168/AGG.2017.0017
journal homepage: https://www.irsm.cas.cz/acta

ORIGINAL PAPER

GEOMETRIC DEFORMATION ANALYSIS IN FREE GEODETIC NETWORKS: CASE STUDY FOR FRUŠKA GORA IN SERBIA

Zoran SUŠIĆ [1], Mehmed BATILOVIĆ [1]*, Toša NINKOV [1], Vladimir BULATOVIĆ [1], Ivan ALEKSIĆ [2] and Gojko NIKOLIĆ [3]

[1] *Faculty of Technical Sciences, University of Novi Sad, Trg Dositeja Obradovića 6, 21000 Novi Sad, Serbia*
[2] *Faculty of Civil Engineering, University of Belgrade, Bulevar Kralja Aleksandra 73, 11000 Belgrade, Serbia*
[3] *Depratment of Geography, University of Montenegro, Danila Bojovića bb, 81400 Nikšić, Montenegro*

**Corresponding author's e-mail:* mehmed@uns.ac.rs

ARTICLE INFO

Article history:
Received 5 April 2017
Accepted 14 July 2017
Available online 23 August 2017

Keywords:
CDA
Robust estimation
Strain analysis

ABSTRACT

The deformation measurements are performed for the purpose of obtaining information concerning ground movement and objects on the ground within given time intervals. For the purpose of improving conventional models of deformation analysis (CDA) it is desirable to use several different methods and also implement alternative procedures as a further improvement, such as the concept of robust geodetic networks and strain analysis, aimed at obtaining objective information about the movements. In the present paper, in addition to the CDA methods, we also analyze the robust methods in deformation detecting and the method of the strain analysis based on elasticity theory as a supplement to the conventional geometric deformation methods (CDA). The mentioned methods are applied and analysed for the case of a test example of Fruška Gora in Serbia, for which there exist geological and geophysical studies of recent tectonic movements. The measuring results for two measuring epochs concern the GNSS vectors measured by applying the fast static method within closed polygons over a ten-year interval, where only the horizontal movement component is analysed. The efficiency of the applied CDA and robust methods is measured by applying a mean success rate (MSR) by applying Monte Carlo simulations in order to investigate the efficiency of a given methods for a given control network.

1. INTRODUCTION

The traditional geodetic approach in the deformation analysis comprises studying the movements in the surface layer of the Earth's crust and engineering objects (bridges, dams, tunnels, high buildings) in time and space. The surface layers of the Earth's crust are in the state of permanent moving due to various influences, such as level change of under the waters, tectonic phenomena, faults, landslides and the like. A space-time analysis involves two kinds of models. Methods testing the congruence of geometric characteristics of an object in two time epochs are known as congruence test methods. The time aspect is taken implicitly. Models describing the deformation on the basis of a given or supposed function of time, i.e. of velocity, acceleration, etc., are called kinematic models. The kinematic models find a special application in determining the regional movements of the Earth's crust, whereas the congruence models are still applied in strictly geometric deformation analysis of engineering objects. There are studies that focus on the application of kinematic models in landslides monitoring, in comparation with CDA methods (Acar et al., 2008). One of the first methods applying congruence models was developed in 1971 by Pelzer at the Hanover University, whereas for a practical use it was adapted by Niemeier in 1976. In 1987 Caspary developed a method based on the congruence of the points of a geodetic network from two epochs, where, unlike Pelzer's method, he assumes that part of the network points is stable. The method is especially efficient in the presence of a fault between two geological blocks. The method developed at the Delft Universities based on a deformation analysis by applying statistical tests developed by Baarda (Kok, 1982; Heck, 1980). The Karlsruhe method, developed at the University in that city, is based on the individual (independent) adjustment for the preceding and current epochs and their common adjustment. In assuming a datum framework the results of geological and geophysical studies are used. The deformation analysis is carried out by statistical testing the general linear hypothesis. To the adapting of the Karlsruhe method to the modern analysis has been contributed by Heck and Kuntz in 1977, Koch in 1980, Heck in 1983 and by many others. The mathematical model of the Karlsruhe method has been implemented in the modern online tracking system for engineering objects based on the conventional and GNSS measurements (Jäger et al., 2006). The generalized method for the purpose of deformation modelling has been developed at the University of New Brunswick, Canada (Chen, 1983). The generalised method consists of three basic procedures: preliminary identification of the deformation model, estimates of the deformation parameters and diagnostic testing of the deformation models with the final choice of the "best one". The comparative analysis of the conventional methods of

Cite this article as: Sušić Z, Batilović M, Ninkov T, Bulatović V et al.: Geometric deformation analysis in free geodetic networks: case study for Fruška Gora in Serbia. Acta Geodyn. Geomater., 14, No. 3 (187), 341–355, 2017. DOI: 10.13168/AGG.2017.0017

deformation analysis can be found in the literature (Setan and Singh, 2001; Velsink, 2015; Sušić et al., 2015).

Robust estimates are most intensively studied methods in statistics, after publishing the pioneer work of Huber in 1964 (Huber, 1964; Caspary, 2000; Xu, 2005). In 1983 Chen published a robust method Iterative Weighted Similarity Transformation (IWST) at the Brunswick University in Canada (Chen, 1983; Chrzanowski and Chen, 1990). In 1987 Caspary and Borutta have given a detail explanation about three robust methods namely Least Absolute Sum (LAS) method, Danish and M-estimation (Huber). IWST and LAS are based on the S transformation for the purpose of detecting the movement trend of the points. The robust estimation of deformation from observation differences (REDOD and its generalization GREDOD) is especially recommended when the observation plan is completely the same for both measurement epochs in order to keep constant possible non-random errors for one geometric network element in both epochs under control (Nowel and Kamiński, 2014; Nowel, 2015). In the literature one can find applications in deformation analyses of the R-estimation (Duchnowski, 2009 and 2013), as well as of the M_{split} estimation (Wiśniewski, 2009; Zienkiewicz, 2014; Zienkiewicz and Baryla, 2015; Zienkiewicz et al., 2017). CDA methods are based on the LS-estimation and robust methods are based on the robust M-estimation.

Chrzanowski and Chen are the first authors who introduce the concepts of a geometric model based on geodetic measurements only and of physical models including the elasticity theory and solid-body mechanics together with the geodetic data (Chrzanowski and Chen, 1990). In 1981 Welsch implemented a procedure based on the analysis of finite elements and strain analysis founded on geodetic observations. Under the influence of external forces bodies suffer deformations, change their shapes and volumes. Changes in the shape and volume, i.e. deformations of a body, are determined on the basis of displacing of every point of the body. Movements of an arbitrary point are due to the movements of the body treated as a rigid body (translation and rotation), as well as to the pure body deformation. The application of the finite-elements method for the strain analysis is implemented after realisation of the geodetic measurements and geodetic-network adjustment for two or more epochs. The complete information on the behaviour of an object exposed to external forces is provided from the deformation components such as translation, rotation and distortion. Namely, the strain analysis serves for the purpose of identifying distortion, i.e. of identifying characteristic forms of terrain motions, such as the compressive, extensive or transcurrent ones. The modern interpretation of strain-model application in geodynamic studies can be found in the following literature (Talich, 2007; Hackl et al., 2009; Deniz and Ozener, 2010; Bogusz et al., 2013; Araskiewicz et al., 2016).

Analogous testings with analysis of two measured epochs can be found in the available literature (Caspary and Borutta, 1987; Caspary et al., 1990; Caspary, 2000; Setan and Singh, 2001; Nowel and Kamiński, 2014; Nowel, 2015). The results of the empirical examining of the CDA method efficiency can be found in Hekimoglu et al. (2010), where the MSR-factor efficiency is examined by applying Monte Carlo simulations. Nowel (2016a) carries out an empirical examination of the efficiencies of various weight functions, for the GREDOD method by applying MSR factor but the conclusions of that research can also concern the IWST method.

2. MOTIVATION

The Republic of Serbia from the global point of view of geodynamics belongs to a part of the Eurasian plate with its northern part belonging to the Panonian Basin (area of Vojvodina) and the central and southern parts in the region of the Dinarides. Fruška Gora as mountain in northwestern Serbia and one of the most interesting areas for the evolution of the Europe–Adria collision zone in terms of orogenic and back-arc interactions is the southern part of the Pannonian Basin near the junction between the Carpathians and Dinarides (Toljić et al., 2013). Fruška Gora is situated south of Novi Sad, on the right bank of the Danube River. It is an east-west extending horst that is bounded by two regional normal faults in the North and South, respectively (Lesić et al., 2007).

Republic Geodetic Authorithy of Serbia has established passive geodetic reference network on whole teritory of Serbia in purpose of forming Serbian spatial reference system SRB_ETRS89. This is not specialized geodynamic network with long continuous interval of observation. However, since at the territory of investigation (Fruška Gora, autonomous province of Vojvodina) so far there was no study dealing with horizontal movements, which were based on geodetic measurements, realization of two times measured network in the ten years interval (2002-2012), for the first time correlation with the geological structures became possible. The points of the passive reference network are uniformly distributed over the region under study with a spatial resolution of about 10 kilometers (Figure 1). In geographic coordinates the research area is located between 44.7 and 45.4 degrees north latitude, and between 19.2 and 20.3 degrees east longitude.

Measurements within the passive geodetic reference network were realized using two-frequency receivers made by Trimble manufacturer used in both first and second campaign. To ensure maximum consistency of observations, the same receivers and antennas were used at each network station in all two campaigns. The measuring results in the two measuring epochs are the GNSS vectors, which are measured by using the fast static method within closed polygons, over approximately a ten-year interval, where the analysis concerns the two-dimensional component only. The time interval at all points is within 90-120 minutes. The point disposition provides

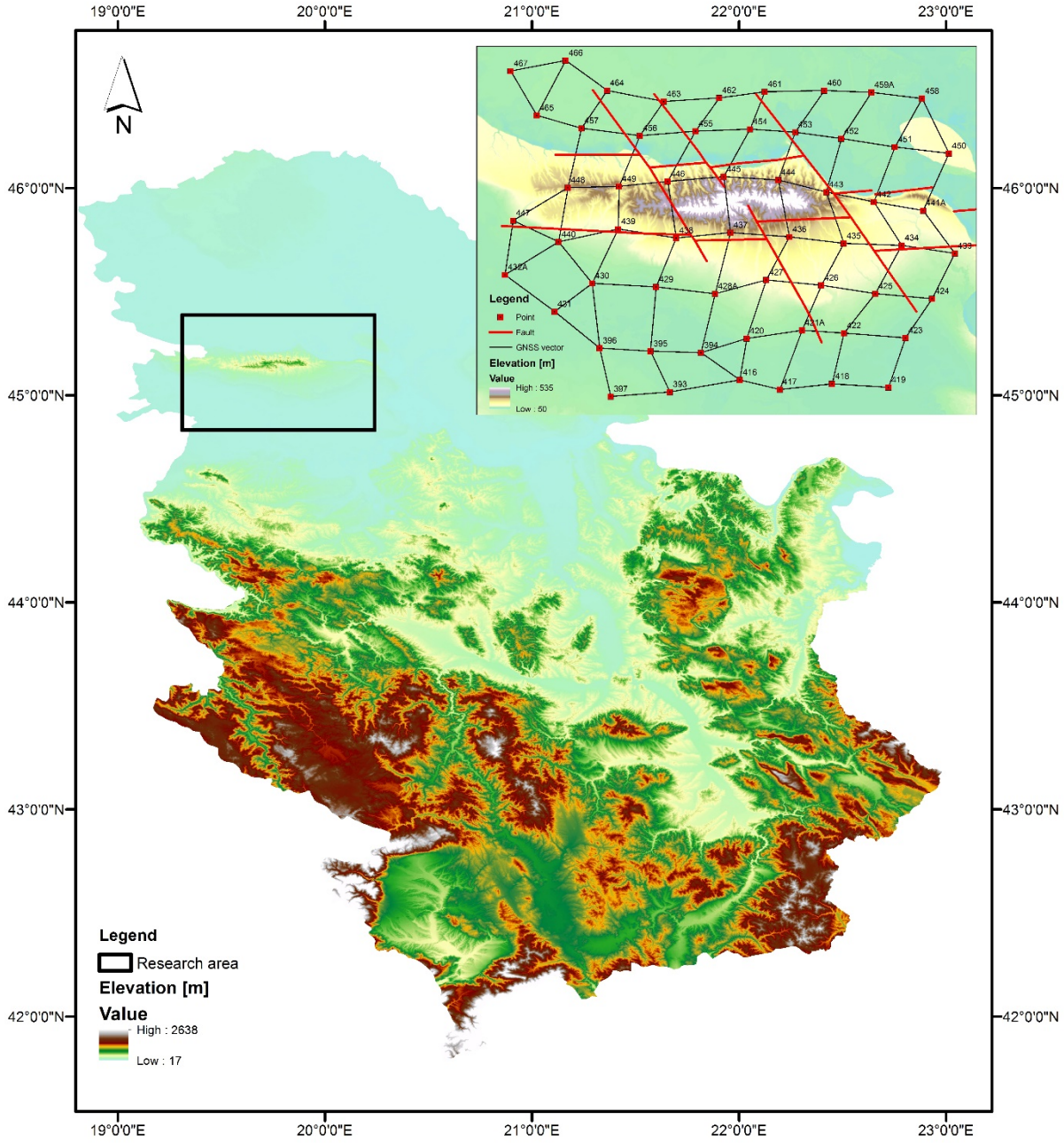

Fig. 1 Fruška Gora shown in the DEM of the Serbia area (dark frame); observations plan of GNSS vectors in passive geodetic network configuration (right); the faults separating significant neotectonic blocks and zones (Marović et al., 2007).

a very good geometry as a prerequisite for a successful application of the deformation analysis. The realization of measurements and vector processing are carried out by the Republic Geodetic Authority of Serbia. The vector processing is done within the closed polygon systems where only linearly independent vectors are taken into account. The quality of the measurements is verified if closing of the polygons is under the limit for allowed deviations of 1 ppm. The spatial coordinates differences subjected to processing are the input parameters for adjustment of measuring results by applying least squares and deformation analysis. The first step is the independent, free adjustment of both measuring epochs aimed at eliminating gross and systematic errors. In order to avoid the influence of different in datum of both epochs on the global network congruence test from two epochs, the displacements and the corresponding variance covariance matrices are transformed into the same datum of both epochs by applying the S transformation. This study aimed to analyse the coordinate differences between the adjusted coordinates obtained from GPS observations in 2002 and the adjusted coordinates obtained from the GNSS observations in 2012 and to compute strain accumulation of the corresponding area by finite element model.

3. DATA AND METHODS

The projecting of a geodetic network for the needs of deformation analysis includes considering the type and size of the deformations which can be detected through the analysis. The deformation measurements can be subject to various error sources, which are due to the imperfection of the equipment, atmospheric conditions and others. In many cases, by applying some of the well-known methods (Baarda, 1968; Pope, 1976) measurements subject to gross errors are identified and eliminated, although sometimes, in spite of the applied procedures, a correct identification misses, which is reflected in the objectivity of the deformation analysis procedure. Namely, in order to make a clear distinction between stochastic variations in the measured values and a deformation it is natural to use the concept of a minimal detectable value which can be "surely" detected following the significance level chosen in the present study (α = 0.05) and test power (1-β = 0.80; β – type II error probability). In the present study we use the following methods of deformation analysis: Pelzer, Karlsruhe, robust methods and strain analysis. By applying the mean success rate (MSR) the total efficiency coefficient for the applied CDA and robust methods, including different variants of the number of unstable points is calculated. The study is aimed at comparing the efficiency of deformation analysis methods (MSR) based on the conventional approach of congruence model and common adjustment for both measuring epochs, methods based on the robust M-estimation with additional calculations of the strain analysis parameters from the finite elements. These models are applied on the test example of Fruška Gora in Serbia, where some geological and geophysical examinations concerning recent tectonic movements have been done, so that in the discussion there is also a short part about the correlation of independent multidisciplinary studies (Sušić et al., 2016). The complete treatment is performed in the specially projected software package MatGeo in the framework of the Matlab programme, which has been developed in the internal surroundings of the Faculty of Technical Sciences in Novi Sad. For the needs of the present study in this software algorithm of all deformation analysis methods mentioned above are implemented. For the purpose of controlling we carry out an independent treatment of measurements in the commercial software package Star*Net 8.1 by applying the *Least Squares method* of indirect adjustment with datum transformation in the solution with a minimal trace of the variance-covariance matrix for all points. The adjusted coordinates with the corresponding variance-covariance matrices for both measuring epochs are transformed into the same datum. A review of theoretical models used in the present study is given in the following text.

3.1. PELZER'S METHOD

The method is based on examination of the congruence of the coordinates of the network points; it is applied in a few steps. In the first step the homogeneity of measurement accuracy for two epochs is examined, where the *a posteriori* equality of the dispersion factors $\hat{\sigma}_{0_1}^2$ and $\hat{\sigma}_{0_2}^2$ from the two epochs, by using Fischer's test, is examined. If the measurement accuracy is homogeneous, then the unified *a posteriori* dispersion factor is determined:

$$\hat{\sigma}_0^2 = (f_1\hat{\sigma}_{0_1}^2 + f_2\hat{\sigma}_{0_2}^2)/f\,,\ f = f_1 + f_2 \tag{1}$$

where f_1 and f_2 are the numbers of degrees of freedom in the preceding and current measurement epochs, f is the number of degrees of freedom from both epochs.

In the second step the network congruence in the two measuring epochs is examined (Pelzer, 1971; Sušić et al., 2015):

$$T = \frac{\hat{\mathbf{d}}^T\mathbf{Q}_{\hat{\mathbf{d}}}^+\hat{\mathbf{d}}}{h\hat{\sigma}_0^2} \sim F_{h,f} \tag{2}$$

where $\hat{\mathbf{d}} = \hat{\mathbf{x}}_2 - \hat{\mathbf{x}}_1$ is the displacement vector, $\hat{\mathbf{x}}_1, \hat{\mathbf{x}}_2$ is vector of adjusted coordinates in the preceding and current measurement epochs, respectively, $\mathbf{Q}_{\hat{\mathbf{d}}} = \mathbf{Q}_{\hat{\mathbf{x}}_1} + \mathbf{Q}_{\hat{\mathbf{x}}_2}$ the cofactor displacement matrix, $\mathbf{Q}_{\hat{\mathbf{x}}_1}$ and $\mathbf{Q}_{\hat{\mathbf{x}}_2}$ the cofactor matrices of unknown parameters from the preceding and current measuring epochs, $h = rank(\mathbf{Q}_{\hat{\mathbf{d}}})$ and $\hat{\sigma}_0^2$ the unified *a posteriori* dispersion factor. If $T \le F_{1-\alpha,h,f}$, the network is congruent in the two epochs, otherwise the network is not congruent in the two epochs.

When the network is not congruent in the two epochs, in the third step one examines the congruence of the points of the potential reference network. For this purpose one decomposes the displacement vector $\hat{\mathbf{d}}$ and pseudo-inverse of the cofactor displacement matrix $\mathbf{Q}_{\hat{\mathbf{d}}}^+$ in the following way:

$$\hat{\mathbf{d}} = \begin{bmatrix}\hat{\mathbf{d}}_S \\ \hat{\mathbf{d}}_O\end{bmatrix} \qquad \mathbf{Q}_{\hat{\mathbf{d}}}^+ = \mathbf{P}_{\hat{\mathbf{d}}} = \begin{bmatrix}\mathbf{P}_{SS} & \mathbf{P}_{SO} \\ \mathbf{P}_{OS} & \mathbf{P}_{OO}\end{bmatrix} \tag{3}$$

where the designation S is referred to the potential reference points of the network, the designation O to the points interpreting the object. The test statistics is (Pelzer, 1971; Sušić et al., 2015):

$$T = \frac{\hat{\mathbf{d}}_S^T\bar{\mathbf{P}}_{SS}\hat{\mathbf{d}}_S}{h_S\hat{\sigma}_0^2} \sim F_{h_S,f} \tag{4}$$

where we have $\bar{\mathbf{P}}_{ss} = \mathbf{P}_{SS} - \mathbf{P}_{SO}\mathbf{P}_{OO}^{-1}\mathbf{P}_{OS}$ and $h_S = rank(\bar{\mathbf{P}}_{ss})$. If $T \le F_{1-\alpha,h_S,f}$, the potential reference points of the network are congruent in the time interval between the two epochs.

If the potential reference points of the network are not congruent in two epochs ($T > F_{1-\alpha,h_S,f}$), it is necessary to localise the unstable points of the potential reference network. The point-displacement vector for the potential reference network $\hat{\mathbf{d}}_S$ and the corresponding matrix $\bar{\mathbf{P}}_{ss}$ are decomposed in the following way:

$$\hat{\mathbf{d}}_S = \begin{bmatrix}\hat{\mathbf{d}}_F \\ \hat{\mathbf{d}}_B\end{bmatrix} \qquad \bar{\mathbf{P}}_{SS} = \begin{bmatrix}\mathbf{P}_{FF} & \mathbf{P}_{FB} \\ \mathbf{P}_{BF} & \mathbf{P}_{BB}\end{bmatrix} \tag{5}$$

where the designation F is referred to the points regarded as conditionally stable and the B one to the points regarded as conditionally unstable. For each point one determines the average non-fitting (Pelzer, 1971; Sušić et al., 2015):

$$\theta_i^2 = \frac{\bar{\mathbf{d}}_B^T \mathbf{P}_{BB} \bar{\mathbf{d}}_B}{h_B}, \ (i = 1,2, \dots, k) \tag{6}$$

where we have $\bar{\mathbf{d}}_B = \hat{\mathbf{d}}_B + \mathbf{P}_{BB}^{-1}\mathbf{P}_{BF}\hat{\mathbf{d}}_F$ and $h_B = rank(\mathbf{P}_{BB})$. The point with maximum average non-fitting θ_i^2 is regarded as unstable and as such it is omitted from the set of the potential reference points. For the rest of $(k-1)$ potential reference network points the congruence examining procedure is repeated by carrying out the second and third steps until for a network part the congruence hypothesis is accepted.

In the fourth step one examines the congruence of points on the object. The displacement vector $\hat{\mathbf{d}}$ of the pseudo-inverse cofactor displacement matrix $\mathbf{Q}_{\hat{\mathbf{d}}}^{+}$ is decomposed in the following way:

$$\hat{\mathbf{d}} = \begin{bmatrix} \hat{\mathbf{d}}_F \\ \hat{\mathbf{d}}_O \end{bmatrix} \qquad \mathbf{Q}_{\hat{\mathbf{d}}}^{+} = \mathbf{P}_{\hat{\mathbf{d}}} = \begin{bmatrix} \mathbf{P}_{FF} & \mathbf{P}_{FO} \\ \mathbf{P}_{OF} & \mathbf{P}_{OO} \end{bmatrix} \tag{7}$$

where the designation F is referred to the stable network points, the O one to the unstable points and the points on the object. The test statistics is (Pelzer, 1971; Sušić et al., 2015):

$$T = \frac{\bar{\mathbf{d}}_O^T \mathbf{P}_{OO} \bar{\mathbf{d}}_O}{h_O \hat{\sigma}_0^2} \sim F_{h_O,f} \tag{8}$$

where we have $\bar{\mathbf{d}}_O = \hat{\mathbf{d}}_O + \mathbf{P}_{OO}^{-1}\mathbf{P}_{OF}\hat{\mathbf{d}}_F$ and $h_O = rank(\mathbf{P}_{OO})$. If $T \leq F_{1-\alpha,h_O,f}$, the points on the object are congruent within the time interval between the two epochs.

3.2. MINIMAL DETECTABLE DEFORMATION

For the geodetic control networks, which are projected, to determine displacements of points, with defined plan measurements and *a priori* standard σ_0, level of significance α and power of test $1-\beta$, it is natural to use the concept of the minimal detectable bias to evaluate the type and size of deformation which can be detected by the analysis. To establish a measure for the quality of the monitoring network, the sensitivity analysis is established (Pelzer, 1971; Aydin, 2012). In the context of deformation analysis, we shall talk about the minimal detectable deformation (MDD) (Prószyński, 2010; Velsink, 2015).

From a separate adjustment, one obtains the parameter estimates $\hat{\mathbf{x}}_1$ and $\hat{\mathbf{x}}_2$ and their cofactor matrices, $\mathbf{Q}_{\hat{\mathbf{x}}_1}$ and $\mathbf{Q}_{\hat{\mathbf{x}}_2}$. The global congruence test of the null hypothesis:

$$H_0: E(\mathbf{d}) = 0 \tag{9}$$

is given by the test statistics (Pelzer, 1971):

$$T_{|H_0} = \left.\frac{\mathbf{d}^T \mathbf{Q}_{\mathbf{d}}^{+} \mathbf{d}}{h\hat{\sigma}_0^2}\right|_{H_0} \sim F_{h,f} \tag{10}$$

where $\mathbf{d} = \hat{\mathbf{x}}_2 - \hat{\mathbf{x}}_1$ is the displacement vector, $\mathbf{Q}_{\mathbf{d}} = \mathbf{Q}_{\hat{\mathbf{x}}_1} + \mathbf{Q}_{\hat{\mathbf{x}}_2}$ is the cofactor displacement matrix, $f = f_1 + f_2$ the unified number of degrees of freedom and $h = rank(\mathbf{Q}_{\mathbf{d}})$.

If H_0 holds, T follows the central F-distribution. For an alternative hypothesis

$$H_a: E(\mathbf{d}) \neq 0 \tag{11}$$

the statistics T is distributed according to the non-central F-distribution with the non-centrality parameter:

$$\lambda = \frac{\mathbf{d}^T \mathbf{Q}_{\mathbf{d}}^{+} \mathbf{d}}{\sigma_0^2} \tag{12}$$

Now the test power is defined as the probability $1-\beta$ which will lead $\mathbf{d}$ to the rejection of H_0 at a level of significance α. If a 1-dimensional test is performed and the size is chosen as $\alpha = 0.05$ and the test power $1-\beta = 0.80$, $f = 2$, a value of non-centrality parameter in $\chi^2(f)$ is $\lambda_0 = 32$ (Aydin, 2012).

If the non-centrality parameter λ should be equal to the theoretical value $\lambda_0 = f(h, \alpha_0, \beta_0)$ in the previous term (Baarda, 1968), then one can write:

$$\mathbf{d}^T \mathbf{Q}_{\mathbf{d}}^{+} \mathbf{d} = \sigma_0^2 \lambda_0 \tag{13}$$

Since the displacement vector can be expressed as:

$$\mathbf{d} = a\mathbf{g} \tag{14}$$

where a is a scalar to be determined and $\mathbf{g}$ is the form vector, i.e. the relative magnitude of movements which is known. If expression in Eq. (14) is substituted in Eq. (13), the minimum value of the displacement which can be detected in the direction of a given vector $\mathbf{g}$ can be obtained:

$$a_{min} = \sigma_0 \sqrt{\frac{\lambda_0}{\mathbf{g}^T \mathbf{Q}_{\mathbf{d}}^{+} \mathbf{g}}} \tag{15}$$

Further, based on expression in Eq. (14) one can determine the minimum deformation which can be detected in the direction of a given vector $\mathbf{g}$:

$$\mathbf{d}_{min} = a_{min}\mathbf{g} \tag{16}$$

It is very important to determine the directions in which one will obtain the weakest estimate of unknown parameters. These directions are actually the directions of the largest axis of the confidence ellipsoid (ellipse).

3.3. KARLSRUHE METHOD

In the first step one performs the independent adjustment of the measured quantities for each epoch following the indirect adjustment The Karlsruhe method is based on the independent adjustment of individual measuring epochs and their common adjustment method. From every individual adjustment the quadratic form $\Omega_i = (\mathbf{v}^T \mathbf{P} \mathbf{v})_i$ is determined, whereas the common quadratic form is obtained by adding the quadratic forms for the individual epochs

$\Omega_0 = \sum \Omega_i$. The total number of degrees of freedom b is obtained by adding the numbers of degrees of freedom b_i from the adjustment of the individual epochs.

In the second step the common adjustment for both measuring epochs is done, where the vector of unknown coordinates $\mathbf{x}$ is decomposed in the following way:

$$\mathbf{x}^T = [\mathbf{z}^T \quad \mathbf{x}_1^T \quad \mathbf{x}_2^T] \tag{17}$$

where $\mathbf{z}$ is the subvector of the points which are assumed to be stable, whereas $\mathbf{x}_1$ and $\mathbf{x}_2$ are the subvectors of the points which are assumed to be unstable. The quadratic form Ω_z obtained from the common adjustment contains information about the measurement errors and displacement of the unstable points. The quadratic form Ω_h can be presented in the following way:

$$\Omega_\mathrm{h} = \Omega_\mathrm{z} - \Omega_0 \tag{18}$$

For the purpose of stability examination for conditionally stable network points one forms the test statistics (Heck, 1983; Sušić et al., 2015):

$$T = \frac{\Omega_\mathrm{h}/f}{\Omega_0/b} \sim F_{1-\alpha,f,b} \tag{19}$$

where $f = (k-1)np_0 - d$, k number of epochs, n dimension of geodetic network, p_0 number of conditionally stable points and d rank defect of the design matrix $\mathbf{A}$. If $T \leq F_{1-\alpha,f,b}$, then the set of conditionally stable points contains no unstable points.

When in the set of conditionally stable points there are unstable points ($T > F_{1-\alpha,f,b}$), it is necessary to indicate such points. To this end common adjustments are repeated where from each of them one conditionally stable point is successively omitted. The adjustment for which the quadratic form is minimal indicates that the point omitted in it should be regarded as unstable. This point is definitively omitted from the set of conditionally stable points and the whole procedure is repeated without it. The procedure is iteratively repeated until the condition $T \leq F_{1-\alpha,f,b}$ is satisfied.

The deformation localisation is carried out for every point, the test statistics (20) is (Heck, 1983; Sušić et al., 2015):

$$T_i = \frac{\hat{\mathbf{d}}_i^T \mathbf{Q}_{\hat{\mathbf{d}}_i}^{-1} \hat{\mathbf{d}}_i}{h_i \hat{\sigma}_0^2} \sim F_{1-\alpha,h_i,b} \tag{20}$$

where: $\hat{\mathbf{d}}_i = \mathbf{B}^T\hat{\mathbf{x}}$ is the displacement vector, $\mathbf{Q}_{\hat{\mathbf{d}}_i} = \mathbf{B}^T\mathbf{Q}_{\hat{\mathbf{x}}}\mathbf{B}$ cofactor displacement matrix, $\mathbf{B}^T = [0 \ \ldots \ -\mathbf{I}_i \ldots \ \mathbf{I}_i \ldots \ 0]$ where $\mathbf{I}_i$ is the identity matrix, $\hat{\mathbf{x}}^T = [\hat{\mathbf{z}}^T \quad \hat{\mathbf{x}}_1^T \quad \hat{\mathbf{x}}_2^T]$ is adjusted coordinates vector from the joint adjustment of both epochs, $\hat{\sigma}_0^2 = (b_1\hat{\sigma}_{0_1}^2 + b_2\hat{\sigma}_{0_2}^2)/(b_1 + b_2)$ the *a posteriori* unified dispersion factor and $h_i = rank(\mathbf{Q}_{\hat{\mathbf{d}}_i})$. If $T_i \leq F_{1-\alpha,h_i,b}$, the point is stable, otherwise it is unstable.

3.4. ROBUST METHODS

Robust methods are used in estimating the trend of point displacing and have a wide application in deformation detection. The best known methods from this group are the IWST method, which satisfies the condition of minimum sum of displacement components module (Chen, 1983; Setan and Singh, 2001), which differs only by weight function (L1-norm function for the displacement vector components, L1-norm function for the displacement lengths and Huber function for the displacement vector components (Caspary and Borutta, 1987; Setan and Singh, 2001, Nowel and Kamiński, 2014). Robust methods are based on the S transformation (Helmert's similarity transformation):

$$\left.\begin{aligned} \hat{\mathbf{d}}^{(k)} &= \mathbf{S}^{(k)}\mathbf{d} \\ \mathbf{Q}_{\hat{\mathbf{d}}}^{(k)} &= \mathbf{S}^{(k)}\mathbf{Q}_{\mathbf{d}}(\mathbf{S}^{(k)})^T \\ \mathbf{W}^{(k+1)} &= diag(\ldots, \omega_i^{(k+1)}, \ldots) \end{aligned}\right\}_{k=1,2,\ldots} \tag{21}$$

where $\mathbf{d} = \hat{\mathbf{x}}_\mathbf{2} - \hat{\mathbf{x}}_\mathbf{1}$ is the displacement vector, $\mathbf{Q}_\mathbf{d} = (\mathbf{Q}_{\hat{\mathbf{x}}_1} + \mathbf{Q}_{\hat{\mathbf{x}}_2})$ cofactor displacement matrix, $\mathbf{S}^{(k)} = \mathbf{I} - \mathbf{H}(\mathbf{H}^T\mathbf{W}^{(k)}\mathbf{H})^{-1}\mathbf{H}^T\mathbf{W}^{(k)}$ S transformation matrix, $\mathbf{I}$ unit matrix, $\mathbf{H}$ matrix of datum conditions and $\mathbf{W}$ weight matrix. For the purpose of forming the weight matrix $\mathbf{W}$ any weight function from the robust estimates group M can be used. In the first iteration ($k = 1$) the weight matrix is treated as the unit one ($\mathbf{W}^{(k=1)} = \mathbf{I}$).

For 2D networks, in the subsequent iterations the weights are formed following the expressions:

$$\omega_i^{(k+1)} = 1/\sqrt{\left(\hat{d}_{x_i}^{(k)}\right)^2 + \left(\hat{d}_{y_i}^{(k)}\right)^2} \qquad \text{L1-norm for the displacement lengths} \tag{22}$$

$$\omega_i^{(k+1)} = 1/\left|\hat{d}_i^{(k)}\right| \qquad \text{L1-norm for the displacement vector components} \tag{23}$$

In the course of iterative procedure from Eq. (21) some values $d_i^{(k)}$ (or $d_{x_i}^{(k)}, d_{y_i}^{(k)}$) can become close to zero, causing in this way a numerical instability in the weight determination. For this reason in practice, expressions in Eqs. (22) and (23) are modified in the following way:

$$\omega_i^{(k+1)} = 1/(\sqrt{\left(\hat{d}_{x_i}^{(k)}\right)^2 + \left(\hat{d}_{y_i}^{(k)}\right)^2} + c) \qquad \text{L1-norm for the displacement lengths} \tag{24}$$

$$\omega_i^{(k+1)} = 1/(\left|\hat{d}_i^{(k)}\right| + c) \qquad \text{L1-norm for the displacement vector component} \tag{25}$$

where c is the tolerance value (for instance 0.0001m). Huber's weight function has the following form:

$$\omega_i^{(k+1)} = \begin{cases} 1 & \text{for } \left|\hat{d}_i^{(k)}\right| \le q_i \\ q_i / \left|\hat{d}_i^{(k)}\right| & \text{otherwise} \end{cases} \quad (26)$$

where $q_i = a\hat{\sigma}_{\hat{d}_i}$ is the tuning constant, a a suitable factor (for instance, $a = 2$) and $\hat{\sigma}_{\hat{d}_i}$ is the standard deviation estimate for the corresponding component of the displacement vector $\hat{d}_i$ ($\hat{\sigma}_{\hat{d}_{y_i}}$ or $\hat{\sigma}_{\hat{d}_{x_i}}$).

It is important to say that only the points of the potential reference network can be included in optimization process given in Eq. (21), then the weights of the points on the object must be equal to zero. Iterative procedure given in Eq. (21) is continued until the module of the differences between successively transformed displacement vectors $\left|\hat{\mathbf{d}}^{(k+1)} - \hat{\mathbf{d}}^{(k)}\right|$ are smaller than the adopted tolerance value c. The displacement vector and its corresponding cofactor matrix from the final iteration are used for the purpose of examining the stability of the network points.

The examination of point stability is done by applying the *single-point* test:

$$T_i = \frac{(\hat{\mathbf{d}}_i^{(k+1)})^T (\mathbf{Q}_{\hat{\mathbf{d}}_i}^{(k+1)})^{-1} \hat{\mathbf{d}}_i^{(k+1)}}{h_i \hat{\sigma}_0^2} \sim F_{1-\alpha,h_i,f} \quad (27)$$

where: $\hat{\mathbf{d}}_i$ is the displacement vector, $\mathbf{Q}_{\hat{\mathbf{d}}_i}$ cofactor displacement matrix, f unified number of degrees of freedom for all measurement epochs, $h_i = rank(\mathbf{Q}_{\hat{\mathbf{d}}_i})$ and $\hat{\sigma}_0^2$ unified *a posteriori* dispersion factor. If $T_i \le F_{1-\alpha,h_i,f}$, the point is stable, otherwise ($T_i > F_{1-\alpha,h_i,f}$) the point is unstable.

Detailed explanations concerning the robust methods can be found in contributions of the following authors: (Chen, 1983; Caspary and Borutta, 1987; Setan and Singh, 2001; Nowel and Kamiński, 2014; Nowel, 2015, 2016a, 2016b).

3.5. MEAN SUCCESS RATE

A deformation analysis procedure is regarded as efficient if all actually displaced points are identified as unstable by applying the corresponding deformation analysis methods. In order to measure the efficiency of CDA and robust methods, it is necessary to be pre-informed about point displacement. Obtaining such an information with certainty in practice is not possible, but point displacement can be simulated. The application efficiency in the case of different methods can be measured by means of the mean success rate (MSR) factor (Hekimoglu et al., 2010; Nowel, 2016a). MSR is a very good empirical efficiency measure for the deformation analysis methods, which is calculated on the basis of a large number of simulated observation sets (zero and control measuring epochs). The simulations are done by applying the Monte Carlo method.

In generating simulated measurements of displacements of geodetic-network points the directions (for 2D and 3D networks) and magnitudes of the displacement vectors are chosen at random. For 2D networks in simulating magnitudes of the displacement vectors it is not suitable to use confidence ellipses, because the radius magnitude of a confidence ellipse is not constant and azimuth dependent (Nowel, 2016a). The circle the area of which is equal to that of confidence ellipse is very suitable in simulating the magnitudes of point displacements. The radius of the corresponding confidence circle is given as $r_i = \sqrt{ab}$, where a and b are the semiaxes major and minor of the confidence ellipse, respectively. The formulae yielding the elements of confidence ellipses can be found in (Hekimoglu et al., 2010; Kamiński and Nowel, 2013). In order to protect the displacement magnitudes almost completely from the stochastic effect influence the significance level of confidence ellipses should be low (Hekimoglu et al., 2010; Nowel, 2016a). The magnitudes of the displacement vectors for the points take the values from an interval $[r_i, lr_i]$, where l is the value defining the upper interval limit ($l > 1$). The azimuths of the simulated displacement vectors take the values from an interval $[0, 2\pi]$. In practice the deformation measurements are subject to an influence of the random errors so that it is necessary to simulate the presence of the latter ones. On the basis of simulated random errors and displacement vectors the simulated observations for the zero and control epochs are formed in the following way:

$$\mathbf{l}_1^{obs} = \mathbf{l} + \mathbf{e}_1, \mathbf{l}_2^{obs} = \mathbf{l} + \mathbf{e}_2 + \mathbf{A}\mathbf{d} \quad (28)$$

where $\mathbf{l}$ is the vector of *theoretical observations* (it can be determined on the basis of approximate point coordinates), $\mathbf{e}_1$ and $\mathbf{e}_2$ are the vectors of simulated measuring errors in the zero and control measurement epochs, $\mathbf{A}$ design matrix and $\mathbf{d}$ the vector of simulated displacements. In order to achieve a reliability examination concerning the deformation analysis method as efficient as possible, it is necessary to form independently a large number of sets of simulated observations according to Eq. (28). The deformation analysis, by applying an adequate method, is carried out for every set of simulated observations. Once all points at which the displacements are simulated are identified as unstable, the procedure is regarded as successful. The MSR criterion can be represented by the following expression (Nowel, 2016a):

$$MSR(n_d) = S/N \quad (29)$$

where n_d is the number of points at which the displacements are simulated, S the number of sets of simulated observations for which the deformation analysis procedure proves successful and N the total number of simulated observation sets. The mean success rate is given as the number of successes divided by the number of experiments (Hekimoglu and Koch, 1999; Hekimoglu et al., 2010; Nowel, 2016a). In the reliability examination procedure concerning a deformation analysis method it is necessary to determine the MSR coefficient for different values of n_d, in order to determine the total

model efficiency. A more detailed explanation of MRS can be found in the literature (Hekimoglu and Koch, 1999; Hekimoglu and Erenoglu, 2007; Erenoglu and Hekimoglu, 2010; Nowel, 2016a).

3.6. STRAIN ANALYSIS

By conventional models of deformation analysis a discrete character information is obtained, such as displacements or velocities of the control points, whereas the deformation remains to be a spatially continuous phenomenon. A deformation, freely interpreted, is a change of the size and shape of a body and it is historically related to the studying o f deformable material bodies in the framework of elasticity theory, and later in continuum mechanics. The principles of strain analysis are applicable if the observed region or object is covered by the deformation model (geodetic network) which can be observed as a continuum deformation under load (Welsch, 1983; Dermanis and Livieratos, 1983; Caspary, 2000). In geodesy it is most frequently applied for the needs of interpreting the deformations of the Earth's crust where all deformation components are determined (translation, rotation and distortion). In this way a more complete information about the behaviour of the object under study is obtained, which makes the strain analysis suitable in the procedures of deformation monitoring, analysis and interpretation.

When a two-dimensional network is the subject, in the immediate neighbourhood of the points deformations can be modelled by the following expression:

$$\mathbf{d} = \mathbf{Ht} + \mathbf{Edx} \tag{30}$$

where:

$\mathbf{Ht}$ is rigid body displacement

$$\mathbf{E} = \left(\frac{\partial \mathbf{d}}{\partial \mathbf{x}}\right) = \begin{pmatrix} \frac{\partial \mathbf{d}_x}{\partial x} & \frac{\partial \mathbf{d}_x}{\partial y} \\ \frac{\partial \mathbf{d}_y}{\partial x} & \frac{\partial \mathbf{d}_y}{\partial y} \end{pmatrix} = \begin{pmatrix} e_{xx} & e_{xy} \\ e_{yx} & e_{yy} \end{pmatrix}$$

deformation tensor.

The asymmetric matrix $\mathbf{E}$ is decomposed into the sum of the symmetric matrix $\boldsymbol{\varepsilon}$ and oblique-symmetric matrix $\boldsymbol{\omega}$:

$$\mathbf{E} = \frac{1}{2}(\mathbf{E} + \mathbf{E}^T) + \frac{1}{2}(\mathbf{E} - \mathbf{E}^T) = \boldsymbol{\varepsilon} + \boldsymbol{\omega} \tag{31}$$

where $\boldsymbol{\varepsilon}$ is the strain tensor and $\boldsymbol{\omega}$ rotation matrix. The diagonal elements of the matrix $\boldsymbol{\varepsilon}$, ε_{xx} and ε_{yy} are the strain parameters along the coordinate axes. The doubled values of the non-diagonal elements of the matrix $\boldsymbol{\varepsilon}$, $2\varepsilon_{xy} = 2\varepsilon_{yx}$ are equivalent to the angular distortion of the right angle which was originally parallel to the coordinate system axes. The rotation of the rigid body is given by the angle ω_{xy}.

Expression from Eq. (30) is strictly valid only in the differential neighbourhood of the point. If the application of the deformation tensor $\mathbf{E}$ is aimed towards the whole domain of the study, it is necessary to assume the homogeneity of the deformation. This restriction makes the strain analysis unsuitable in many deformation analysis problems. However, in practice the problem can be solved by dividing the network into the finite elements. Then the homogeneity condition is restricted to the inside of the finite element. In order to determine the strain parameters three points are necessary. Therefore, the network can be decomposed into triangle elements.

The results of the strain analysis can be also graphically interpreted. To this end one from the basic strain parameters $(\varepsilon_{xx}, \varepsilon_{xy}, \varepsilon_{yy})$ determines the additional ones (Talich, 2007):

$\Delta = \varepsilon_{yy} + \varepsilon_{xx}$	total dilatation	(32)
$\gamma_1 = \varepsilon_{yy} - \varepsilon_{xx}$	pure shear stress	(33)
$\gamma_2 = 2\varepsilon_{xy}$	engineering shear stress	(34)
$\gamma = \sqrt{\gamma_1^2 + \gamma_2^2}$	total shear stress	(35)
$e_1 = \frac{1}{2}(\Delta + \gamma)$	maximum strain axis	(36)
$e_2 = \frac{1}{2}(\Delta - \gamma)$	minimum strain axis	(37)
$\varphi = \frac{1}{2}\arctan(\gamma_2/\gamma_1)$	azimuth of maximum strain axis	(38)
$\psi = \varphi + \frac{1}{4}\pi$	maximum shear stress direction	(39)

For the needs of the experimental studies in the present work and calculating of the strain parameters we apply the method based on point displacements, the so called X-mehtod (Welsch, 1983). The finite elements method is applied after observations and adjusting the geodetic network in two epochs. The hypotheses about accuracy homogeneity and network congruence from two epochs are realised in the same way as in the case of Pelzer's method, before dividing the network into finite elements (Welsch, 1983).

4. RESULTS

The relative geodetic network whereby the territory of Fruška Gora is covered consists of 57 points. The disposition of the network points is presented in Figure 2. After realising the zero measurement epoch network

points 421, 428, 432, 441 and 459 were destroyed. When the control measurement epoch was realised, the restabilisation of the destroyed points took place. These points are included in the adjusting process of the zero and control, measurements epochs in order to preserve the network geometry. However, these points are not treated in the deformation analysis procedure. The horizontal displacements of the relative network points, calculated, as changes of coordinates acquired from GPS measurements are determined in a local, topocentric system defined by minimal constraints of network.

After confirming the hypothesis about a homogeneous measurement accuracy between the two epochs the deformation analysis is carried out following Pelzer's method, where a network in congruence between the two epochs of measuring is established ($T = 10.446 > F_{0.95,102,184} = 1.325$). Earlier, we must transform, using S-transformation, the coordinates from both epochs to minimum trace datum defined on all the tested points. Only now we can carry out the single point displacement analysis by Pelzer method. In order to identify significantly displaced points a localisation procedure for unstable points is carried out following expressions in Eqs. (5) and (6). On a total of 20 points significant displacements are identified, whereas the rest of the points are identified as non-displaced (stable) between the two epochs. In Table 1 the estimated displacement vectors are given for each point; this is followed by information about the point status (stable or unstable). For the needs of the deformation analysis following the Karlsruhe method a common adjustment of the epoch measurements is done. By applying the Karlsruhe method the network incongruence from the two epochs is also established, on the basis of expression in Eq. (19) ($T = 10.572 > F_{0.95,102,184} = 1.325$). Afterwards a localisation procedure for significantly displaced network points is carried out. The total contains 45 iterations, in the case of points 424, 427, 450, 451, 461, 463 and 464 the congruence on the basis of expression in Eq. (19) is confirmed ($T = 1.184 < F_{0.95,12,184} = 1.805$). These points are declared stable and in the further procedure they are regarded as reference points. For the rest of the points the stability examination is carried out following expression given in Eq. (20). The status information (stable or unstable) and the estimated displacement vectors are given in Table 1.

The most unfavourable case of congruence examination for a point concerns the direction of the semimajor axis of the confidence ellipse because in that direction the determination error for a point position is maximal. On the other hand, the most favourable case of congruence examination for a point concerns the direction of the semiminor axis of the confidence ellipse. On the basis of expressions from Eqs. (15) and (16), for each network point the value for the minimal detectable deformation d_{min} along the semimajor axis of the confidence ellipse is calculated, as well as the corresponding standard deviation $\sigma_{d_{min}}$. The obtained results are given in Table 1.

In addition to Pelzer's and Karlsruhe methods, the three robust methods which differ only by weight function are also applied: L1-norm function for the displacement vector components (L1-norm I), L1-norm function for the displacement lengths (L1-norm II) and Huber function for the displacement vector components. In the case of the robust methods iterative procedure from Eq. (21) is carried out until the module of the difference of successively transformed displacement vectors are under the given tolerance value. The tolerance value assumed here is $c = 0.1$ mm. In this case all network points are included in optimisation process given in Eq. (21) (relative network). The total number of iterations for L1-norm I is 7, for L1-norm II one 5, and for Huber's one 4. The displacement vector and the corresponding cofactor matrix from the last iteration are used for the needs of the stability examination for the network points. The stability examination for the network points, i. e. the identification of significantly displaced points, is carried out according to expression from Eq. (27). The displacement vectors are identified by applying the robust methods as well as using the status information (stable or unstable); this can be seen in Table 2. The displacement vectors obtained by applying CDA and robust methods with absolute and relative confidence ellipses ($\alpha = 0.05$) are presented in Figure 2.

It is important to mention that, in addition to the real results of the measurements performed on the example of Fruška Gora (Tables 1 and 2), the results of the Monte Carlo simulations aimed at efficiency establishing for the applied deformation analysis methods are also given (Table 3). The conception of the MSR efficiency criteria provides insight in the reliability of the deformation analysis methods applied to the test example of Fruška Gora. In order to examine the efficiency of CDA and robust methods applied here we analyses different variants from the standpoint of the number of displaced points n_d. For each variant 5000 different observation sets (zero and control epochs) are simulated according to expression given in Eq. (28). The random measuring errors obey the normal distribution with standard deviations of the performed measurements in the framework of the zero and control epochs. The magnitudes of the simulated displacement vectors are within an interval from r to $3r$, where $r = \sqrt{ab}$, a the semimajor axis of the confidence ellipse and b its semiminor axis, whereas the azimuths of the simulated displacement vectors are between 0 and 2π. The displacement vectors and the random measuring errors are determined by applying the uniform pseudo-random error and normal pseudo-random error generators, in a Matlab programme. The MSR coefficients are determined following expression given in Eq. (29), for each method in the framework of all considered variants.

Table 1 The results of CDA methods of deformation analysis ($\alpha = 0.05, 1-\beta = 0.80$).

Point	Pelzer		Karlsruhe		MDD		Point	Pelzer		Karlsruhe		MDD	
	$\hat{d}$ [mm]	Stable	$\hat{d}$ [mm]	Stable	d_m [mm]	σ_{d_m} [mm]		$\hat{d}$ [mm]	Stable	$\hat{d}$ [mm]	Stable	d_m [mm]	σ_{d_m} [mm]
393	10.1	**Yes**	9.7	**Yes**	41.4	7.3	440	5.2	**Yes**	2.0	**Yes**	36.1	6.4
394	17.8	**No**	17.5	**No**	36.6	6.5	442	7.3	**Yes**	9.0	**Yes**	39.0	6.9
395	18.1	**No**	16.1	**No**	36.9	6.5	443	5.2	**Yes**	1.7	**Yes**	39.1	6.9
396	10.3	**No**	14.0	**No**	35.8	6.3	444	42.9	**No**	43.3	**No**	39.4	7.0
397	21.8	**No**	18.0	**No**	46.7	8.3	445	1.5	**Yes**	1.4	**Yes**	35.8	6.3
416	6.0	**Yes**	4.3	**Yes**	38.0	6.7	446	15.3	**No**	11.7	**No**	38.7	6.9
417	21.8	**No**	17.4	**No**	41.7	7.4	447	8.2	**Yes**	9.0	**Yes**	45.0	8.0
418	7.4	**Yes**	8.7	**Yes**	53.6	9.5	448	3.9	**Yes**	1.6	**Yes**	39.5	7.0
419	6.5	**Yes**	5.5	**Yes**	56.5	10.0	449	3.0	**Yes**	4.9	**Yes**	36.4	6.4
420	7.0	**Yes**	8.3	**Yes**	41.9	7.4	450	10.9	**No**	--	**Yes**	50.5	9.0
422	0.6	**Yes**	6.2	**Yes**	40.2	7.1	451	11.4	**No**	--	**Yes**	42.2	7.5
423	7.2	**Yes**	11.2	**No**	45.7	8.1	452	8.1	**No**	5.9	**Yes**	40.3	7.1
424	5.8	**Yes**	--	**Yes**	45.7	8.1	453	6.0	**Yes**	4.5	**Yes**	40.6	7.2
425	5.1	**Yes**	4.4	**Yes**	37.2	6.6	454	52.9	**No**	50.9	**No**	35.1	6.2
426	3.9	**Yes**	4.8	**Yes**	34.6	6.1	455	6.7	**Yes**	7.8	**Yes**	35.4	6.3
427	0.4	**Yes**	--	**Yes**	34.9	6.2	456	49.9	**No**	53.9	**No**	36.3	6.4
429	10.1	**Yes**	12.3	**Yes**	34.3	6.1	457	26.0	**No**	21.8	**No**	42.2	7.5
430	3.4	**Yes**	3.5	**Yes**	33.9	6.0	458	28.1	**No**	29.0	**No**	45.8	8.1
431	10.5	**Yes**	13.0	**Yes**	38.7	6.9	460	7.9	**Yes**	10.7	**No**	44.5	7.9
433	11.4	**Yes**	12.5	**Yes**	44.4	7.8	461	1.6	**Yes**	--	**Yes**	47.4	8.4
434	16.0	**No**	15.5	**No**	36.4	6.4	462	38.0	**No**	37.3	**No**	53.1	9.4
435	11.1	**No**	8.4	**Yes**	34.5	6.1	463	9.3	**Yes**	--	**Yes**	46.1	8.2
436	3.2	**Yes**	1.7	**Yes**	33.8	6.0	464	9.9	**No**	--	**Yes**	48.8	8.6
437	8.2	**Yes**	9.8	**Yes**	36.6	6.5	465	1.9	**Yes**	11.8	**Yes**	64.0	11.3
438	7.2	**Yes**	3.5	**Yes**	39.4	7.0	466	23.6	**No**	28.7	**No**	63.9	11.3
439	9.6	**Yes**	11.6	**Yes**	36.3	6.4	467	27.1	**No**	44.4	**No**	76.8	13.6

The significance level value was set to $\alpha = 0.001$. The total efficiency of individual methods is also calculated. The obtained results are given in Table 3.

For the purpose of determining the strain parameters the network is divided into finite elements of triangle form wherein the Delaunay triangulation method is applied. For each triangle the basic strain parameters (ε_{xx}, ε_{xy} and ε_{yy}) are determined on the basis of the point displacements between the two epochs. The additional strain parameters are calculated from the basic ones following expressions given in Eqs. (32) to (39). The graphical presentation of the additional strain parameters is given in Figure 3. The total dilatation Δ and the total shear strain γ are illustrated by circle outsides, the minimum and maximum strains e_1 and e_2 by two mutually perpendicular lines. The extension is given in red, the compression in blue and the shear stress in green. In Table 4 are given the significant parameters which concern the strain accumulation for each finite element (triangle).

5. DISCUSSION AND CONCLUSIONS

The experimental example, used here for the purpose of analysing the applications of the CDA methods, robust statistical methods and strain analysis, concerns the passive geodetic reference network in the environment of the Fruška Gora mountain (Province of Vojvodina in the northern part of Serbia). Fruška Gora is, in addition to the Vršac Mountains, the only horst in the south-eastern part of the Pannonian Basin, the character of which is largely flat. In the tectonic sense the Pannonian Basin lies within the Eurasian Plate in the northern part of the boundary zone under the influence of the convergence between the African and Eurasian Plates and the Adriatic Block between them. The recent earthquake on the area of Italy is in favor of numerous studies asserting that the Adriatic Block appears as the main compression transmitter for the African and Eurasian tectonic plates, which to a large extent affects the tectonics of the Central European Region, especially that of the Pannonian Basin. In the Fruška Gora area, the exhumation of the metamorphic core of the mountains occurred along the major faults with E-W orientation (Toljić et al., 2013; Sušić et al., 2016). The present results are in favour of significant point displacements on the northwestern and northeastern slopes of Fruška Gora, which are detected by applying deformation analysis methods (CDA and robust methods). All calculations are carried out with standard values $\alpha = 0.05$ and $1 - \beta = 0.80$. In this case the risk is to declare unstable 5 % of the stable points (type I error) and 20 % of the unstable points to

Table 2 The results of Robust methods of deformation analysis.

Point	L1-norm I		L1-norm II		Huber		Point	L1-norm I		L1-norm II		Huber	
	$\hat{d}$ [mm]	Stable	$\hat{d}$ [mm]	Stable	$\hat{d}$ [mm]	Stable		$\hat{d}$ [mm]	Stable	$\hat{d}$ [mm]	Stable	$\hat{d}$ [mm]	Stable
393	9.3	**Yes**	9.3	**Yes**	8.1	**Yes**	440	2.2	**Yes**	2.1	**Yes**	2.2	**Yes**
394	17.1	**No**	17.0	**No**	16.0	**No**	442	5.9	**Yes**	5.8	**Yes**	4.8	**Yes**
395	14.7	**No**	14.7	**No**	13.9	**No**	443	3.4	**Yes**	3.5	**Yes**	4.3	**Yes**
396	16.2	**No**	16.1	**No**	16.2	**No**	444	43.1	**No**	43.2	**No**	42.4	**No**
397	19.4	**No**	19.4	**No**	19.9	**No**	445	1.0	**Yes**	1.0	**Yes**	2.1	**Yes**
416	4.3	**Yes**	4.3	**Yes**	5.4	**Yes**	446	15.4	**No**	15.4	**No**	15.4	**No**
417	16.6	**No**	16.5	**No**	15.6	**No**	447	13.1	**Yes**	13.1	**No**	12.6	**Yes**
418	11.0	**Yes**	11.1	**Yes**	11.5	**Yes**	448	7.2	**Yes**	7.1	**Yes**	7.2	**Yes**
419	10.5	**Yes**	10.5	**Yes**	10.0	**Yes**	449	0.7	**Yes**	0.7	**Yes**	1.7	**Yes**
420	7.9	**Yes**	7.9	**Yes**	8.9	**Yes**	450	14.4	**No**	14.5	**No**	14.7	**No**
422	10.1	**Yes**	10.2	**Yes**	10.2	**Yes**	451	9.7	**Yes**	9.8	**Yes**	10.4	**Yes**
423	16.5	**No**	16.6	**No**	16.4	**No**	452	11.5	**Yes**	11.6	**Yes**	11.8	**No**
424	8.2	**Yes**	8.2	**Yes**	7.6	**Yes**	453	4.1	**Yes**	4.1	**Yes**	3.2	**Yes**
425	8.8	**Yes**	8.9	**Yes**	8.9	**Yes**	454	53.5	**No**	53.4	**No**	53.4	**No**
426	4.3	**Yes**	4.4	**Yes**	5.5	**Yes**	455	5.8	**Yes**	5.8	**Yes**	6.9	**Yes**
427	2.7	**Yes**	2.8	**Yes**	3.8	**Yes**	456	54.8	**No**	54.8	**No**	55.9	**No**
429	11.0	**Yes**	11.0	**Yes**	9.9	**Yes**	457	30.5	**No**	30.4	**No**	30.7	**No**
430	5.1	**Yes**	5.0	**Yes**	4.4	**Yes**	458	19.6	**No**	19.5	**No**	19.7	**No**
431	13.9	**No**	13.8	**Yes**	12.8	**Yes**	460	9.3	**Yes**	9.2	**Yes**	9.1	**Yes**
433	8.8	**Yes**	8.8	**Yes**	9.9	**Yes**	461	3.8	**Yes**	3.7	**Yes**	4.0	**Yes**
434	15.4	**Yes**	15.4	**Yes**	14.3	**Yes**	462	42.7	**No**	42.6	**No**	43.4	**No**
435	11.2	**Yes**	11.2	**Yes**	11.0	**No**	463	10.6	**Yes**	10.6	**Yes**	10.6	**Yes**
436	3.4	**Yes**	3.4	**Yes**	4.5	**Yes**	464	14.4	**No**	14.3	**No**	14.0	**No**
437	8.9	**Yes**	8.9	**Yes**	9.0	**Yes**	465	0.4	**Yes**	0.5	**Yes**	1.6	**Yes**
438	1.5	**Yes**	1.6	**Yes**	2.6	**Yes**	466	22.8	**Yes**	22.8	**Yes**	21.8	**Yes**
439	9.1	**Yes**	9.1	**Yes**	8.2	**Yes**	467	33.1	**No**	33.1	**No**	33.0	**No**

Table 3 The results of MSR calculations (5000 simulation).

Method	$\boldsymbol{MSR}(n_d)$[%] Number of displaced points n_d												Overall efficacy [%]
	0	1	2	3	4	5	6	9	12	15	18	21	
Pelzer	99.9	58.0	74.9	75.1	74.3	70.8	69.4	65.4	61.7	56.4	53.4	48.5	67.3
Karlsruhe	100.0	88.6	78.8	75.4	74.1	70.8	69.2	64.4	59.3	52.4	48.4	41.5	68.6
L1 norm I	98.3	73.8	54.8	47.4	37.4	33.3	25.3	15.7	8.3	5.3	1.9	2.1	33.6
L1 norm II	94.2	74.6	59.9	53.1	48.0	40.9	36.3	24.8	17.2	12.0	8.5	6.1	39.6
Huber	92.5	74.0	60.1	53.5	48.4	42.2	37.8	26.6	18.6	14.0	9.9	7.3	40.4

declare stable (type II error). The results are presented in Tables 1 and 2 and in Figure 2. Thus here we have displacements the magnitude of which exceeds the intensity of the smallest displacement that can be "surely" detected (d_{min}, Table 1). The average value of the minimal detectable deformation along the semimajor axis is equal to 42.3 mm, with an estimated standard deviation of displacement of 7.5 mm. The average of the minimal detectable deformation along the semiminor axis is equal to 26.5 mm, with an estimated standard deviation of displacement of 4.7 mm. The results for the CDA methods (Pelzer's and Karsruhe) show differences at some points. By applying Pelzer's method 20 unstable points are identified, whereas by applying the Karlsruhe one 17 unstable points are identified, just as for the robust methods (L1-nom function for the displacement vector components and L1-nom function for the displacement lengths). On the basis of applying the Huber function for the displacement vector components 18 unstable points are identified.

The MSR coefficients showing the total efficiency of the applied methods are given in Table 3. For the number of displaced points $n_d = 0$, the methods which have the best MSR are Karlsruhe (100.0 %) and Pelzer (99.9 %), to be followed byL1-norm I (98.3 %), L1-norm II (94.2 %) and Huber (92.5 %). As the number of displaced points increases, MSR decreases, especially in the case of the robust methods. In the cases when the number of displaced points is 21, the CDA methods Pelzer (48.5 %) and Karlsruhe (41.5 %) have very close

Table 4 The results of strain analysis.

Finite element	ε_{xx}[μs]	ε_{xy}[μs]	ε_{yy}[μs]	Δ[μs]	γ[μs]	e_1[μs]	e_2[μs]	φ[°]	ψ[°]
8	3.03	-1.69	0.28	3.30	4.35	3.83	-0.53	154.58	199.58
9	4.24	-2.89	6.10	10.35	6.08	8.21	2.14	126.08	171.08
11	-3.75	0.99	-0.49	-4.24	3.82	-0.21	-4.03	74.32	119.32
14	-1.86	0.76	-2.73	-4.59	1.75	-1.42	-3.17	30.23	75.23
40	-2.60	1.44	-2.68	-5.28	2.88	-1.20	-4.08	44.18	89.18
41	-0.33	1.78	-3.70	-4.03	4.91	0.44	-4.47	23.27	68.27
42	0.67	0.38	-3.56	-2.90	4.30	0.70	-3.60	5.13	50.13
46	-2.60	1.64	-0.92	-3.53	3.68	0.08	-3.60	58.57	103.57
47	5.82	0.03	-1.66	4.16	7.49	5.82	-1.66	0.22	45.22
49	-4.23	1.76	2.24	-1.99	7.37	2.69	-4.68	75.75	120.75
52	-7.39	-1.17	0.14	-7.24	7.89	0.32	-7.56	98.63	143.63
53	3.95	1.55	2.06	6.01	3.63	4.82	1.19	29.40	74.40
54	-5.16	-2.90	0.51	-4.65	8.11	1.73	-6.38	112.80	157.80
56	0.80	-1.32	-5.13	-4.33	6.49	1.08	-5.41	168.01	213.01
60	-3.10	2.53	-1.65	-4.74	5.26	0.26	-5.00	53.02	98.02
65	3.01	-5.21	1.72	4.74	10.51	7.62	-2.89	138.54	183.54
67	-0.63	1.34	6.68	6.04	7.78	6.91	-0.87	79.96	124.96

MSR values. When the total efficiency within the chosen interval of r to $3r$ for the number of displaced points between 0 and 21 is observed, the smallest MSR values are for the robust statistical methods: L1 norm I (33.6 %), L1 norm II (39.6 %) and Huber (40.4 %). The CDA methods show a significantly better total MSR, which for Pelzer's method is 67.3 %, whereas for the Karlsruhe method, which is based on the conception of a relative confidence ellipse, MSR is 68.6 %. Similar results with simulated measurements can be found in the literature, where the best MSR is achieved just for the relative confidence ellipse methods with respect to the S-transformations and implicit hypothesis testing (Hekimoglu et al., 2010). The reliability of CDA and robust statistical methods depends on many factors, such as the number of unknowns, number of degrees of freedom, displacement magnitude, number of deformed points, deformation type and the like.

The advantage of the strain analysis as an addition to the CDA and robust methods is that the strain parameters are, on one hand, datum independent quantities, and on the other hand, that they are quantities having a clearly defined both geometric and physical meaning. Translations and rotations have no influence upon the obtained strain tensor parameters, it is only important to provide the same network scale for both measuring epochs. By network division into finite elements (triangles), assuming that they are mutually related, one analyses the whole transforming in this way continual physical systems into discrete ones. In Figure 3 it is possible to see that on the subject area the relative relations of the Earth's crust over a ten-year interval have been changed. On the north-eastern slope of Fruška Gora significant parameters of an extensive character are visible, which follows significant parameters of a compressive character on the north-western side. The purpose of the graphic presentation in the present paper (Figures 2 and 3) is to make it possible to obtain an insight in the spatial distribution of the deformation parameters. The area on the northern fault region of Fruška Gora is characterised by a significant extension along the north-south direction, which can be related to the gravitational descending of the northern block, i.e. to the relative ascending of the southern one. The north-eastern area of Fruška Gora is characterized by the presence of transcurrently right faults where the distribution of local values of the stress field is controlled by the local fault structures. The significant displacement magnitudes and the significant strain parameters, obtained here, are correlated to the reactivated existing structures which have been recognised in earlier geological and geophysical studies (Marović et al., 2007; Matenco and Radivojević, 2012; Toljić et al., 2013).

It is important to say that the geodetic methods of deformation analysis used here provide mainly geometric information about the changes having occurred, where the interpretation of results and identification of causal forces belongs to other kinds of research, such as neotectonic ones, so that geophysical. Monitoring of an engineering object or of an Earth crust area is possible and efficient, only in the case when there exist a given number of reference points beyond the zone of expected deformations. In order to carry out a comprehensive analysis it is necessary to apply as many independent models as possible. This is presented here with the CDA methods, robust statistical techniques and the finite elements method of the strain analysis. The mean success rate, as a measure of efficiency establishing for the models applied in the present paper, can be also used in the process of geodetic network projecting for the needs of monitoring concerning the objects in civil engineering and ground. It is also very

important to know the lower accuracy limit, in order to avoid any negative consequences which to a significant extent can decrease the reliability of information concerning movements of the ground and objects.

In the present paper the GNSS measurements are used, which, even if not realised specially for geodynamic purposes, to a preliminary research, including several distinct models of conventional geometric deformation analysis, robust estimates and strain analysis, can contribute to the understanding of the recent movements in the framework of multidisciplinary studies in the subject field.

ACKNOWLEDGMENTS

The authors express their gratitude to both anonymous reviewers for comments and suggestions made, which was significant for improving the quality of this manuscript. This study was partly supported by the Ministry of Education, Science and Technological Development of the Republic of Serbia (No. III42012). The authors express their gratitude to the Republic Geodetic Authority of Serbia, for putting at their disposal the realized GPS measurements over the passive reference network, which were used for the purposes of the present study.

REFERENCES

Acar, M., Ozludemir, M.T., Erol, S., Celik, R. N. and Ayan, T.: 2008, Kinematic landslide monitoring with Kalman filtering. Natural Hazards and Earth System Sciences, 8, 213–221. DOI: 10.5194/nhess-8-213-2008

Aydin, C.: 2012, Power of global test in deformation analysis. Journal of Surveying Engineering, 138, No. 2, 51–55. DOI: 10.1061/(ASCE)SU.1943-5428.0000064

Araszkiewicz, A., Figurski, M. and Jarosinski, M.: 2016, Erroneous GNSS strain rate patterns and their application to investigate the tectonic credibility of GNSS velocities. Acta Geophysica, 64, No. 5, 1412–1429. DOI: 10.1515/acgeo-2016-0057

Baarda, W.: 1968, A testing procedure for use in geodetic networks. Netherlands Geodetic Commission Publications on Geodesy New Series 2, No. 5.

Bogusz, J., Klos, A., Figurski, M., Jarosinski, M. and Kontny, B.: 2013, Investigation of the reliability of local strain analysis by means of the triangle modeling. Acta Geodyn. Geomater., 10, No. 3 (171), 293–305. DOI: 10.13168/AGG.2013.0029

Caspary, W.F.: 2000, Concepts of network and deformation analysis. The University of New South Wales, Kensington.

Caspary, W.F. and Borutta, H.: 1987, Robust estimation in deformation model. Survey Review, 29, No. 223, 29–45. DOI: 10.1179/sre.1987.29.223.29

Caspary, W.F., Haen, W. and Borutta, H.: 1990, Deformation analysis by statistical methods. Technometrics, 32, No. 1, 49–57. DOI: 10.2307/1269844

Chen, Y.Q.: 1983, Analysis of deformation surveys - A generalized method. Technical Report No. 94, University of New Brunswick, Fredericton, New Brunswick, Canada.

Chrzanowski, A. and Chen, Y. Q.: 1990, Deformation monitoring, analysis and prediction-status report FIG, XIX international congress, Helsinki, 6, 83–97.

Deniz, I. and Ozener, H.: 2010, Estimation of strain accumulation of densification network in Northern Marmara Region, Turkey. Natural Hazards and Earth System Sciences, 10, 2135–2143. DOI: 10.5194/nhess-10-2135-2010

Dermanis, A. and Livieratos, E.: 1983, Applications of deformation analysis in geodesy and geodynamics. Reviews of Geophysics, 21, No. 1, 41–50. DOI: 10.1029/RG021i001p00041

Duchnowski, R.: 2009, Geodetic application of R-estimation - Levelling network examples. Technical Sciences, 12, 135–144.

Duchnowski, R.: 2013, Hodges-Lehmann estimates in deformation analyses. Journal of Geodesy, 87, No. 10, 873–884. DOI: 10.1007/s00190-013-0651-2

Erenoglu, R.C. and Hekimoglu, S.: 2010, Efficiency of robust methods and tests for outliers for geodetic adjustment models. Acta Geodaetica et Geophysica Hungarica, 45, No. 4, 426–439. DOI: 10.1556/AGeod.45.2010.4.3

Hackl, M., Malservisi, R. and Wdowinski, S.: 2009, Strain rate patterns from dense GPS networks. Natural Hazards and Earth System Sciences, 9, 1177–1187. DOI: 10.5194/nhess-9-1177-2009

Heck, B.: 1980, Statistische ausreisserkriterien zur kontrollegeodatischer beobachtungen. VIII Internationalkurs feuer ingenieurvermessung, Zuerich.

Heck, B.: 1983, Das Analzseverfahren des geodatischen instituts der Universitat Karlsruhe. Stand 1983, Deformationsanalysen 1983, Geometrische Analyse und Interpretation von Deformationen Geodattischer Netze, Munchen.

Hekimoglu, S., Erdogan, B. and Butterworth, S.: 2010, Increasing the efficacy of the conventional deformation analysis methods: Alternative strategy. Journal of Surveying Engineering, 136, No. 2, 53–62. DOI: 10.1061/(ASCE)SU.1943-5428.0000018

Hekimoglu, S. and Erenoglu, R.C.: 2007, Effect of heteroscedasticity and heterogeneousness on outlier detection for geodetic networks. Journal Geodesy, 81, No. 2, 137–148. DOI: 10.1007/s00190-006-0095-z

Hekimoglu, S. and Koch, K. R.: 1999, How can reliability of robust methods be measured? Third Turkish-German Joint Geodetic Days, Istanbul, 1, 179–196.

Huber, P.,J.: 1964, Robust estimation of a location parameter.The Annals of Mathematical Statistics, 35, No. 1, 73–101.

Jäger, R., Klber, S. and Oswald, M.: 2006, GNSS/GPS/LPS based Online Control and Alarm System (GOCA) – Mathematical models and technical realisation of a system for natural and geotechnical deformation monitoring and analysis. GEOS.

Kamiński, W. and Nowel, K.: 2013, Local variance factors in deformation analysis of non-homogenous monitoring networks. Survey Review, 45, No. 328, 44–50. DOI: 10.1179/1752270612Y.0000000019

Koch, K.: 1980, Parameterchatzung und Hypothesen test. Bonn.

Kok, J.J.: 1982, Statistical analysis of deformation problems using Baardas testing procedures. Published in Forty

Years of Thought Delft University of Technology, Delft.

Lesić, V., Márton, E. and Cvetkov, V.: 2007, Paleomagnetic detection of Tertiary rotations in the Southern Pannonian Basin (Fruška Gora). Geologica Carpathica, 58, No. 2, 185–193.

Marović, M., Toljić, M., Rundić, Lj. and Milivojević, J.: 2007, Neoalpine tectonics of Serbia. Serbian Geological Society. Ser. Monographie, Belgrade, 87 pp.

Matenco, L. and Radivojević, D.: 2012, On the formation and evolution of the Pannonian Basin: constraints derived from the structure of the junction area between the Carpathians and Dinarides.Tectonics, 31, No. 6. DOI: 10.1029/2012TC003206

Niemeier, W.: 1976, Grundprincip und Rechenformeln einer strengen Analise geodatisher Deformation-smessungen. Hanover.

Nowel, K.: 2015, Robust M-estimation in analysis of control network deformations: Classical and new method. Journal of Surveying Engineering, 144, No. 4. DOI: 10.1061/(ASCE)SU.1943-5428.0000144

Nowel, K.: 2016a, Investigating efficacy of robust M-estimation of deformation from observation differences. Survey Review, 48, No. 346, 21–30. DOI: 10.1080/00396265.2015.1097585

Nowel, K.: 2016b, Application of Monte Carlo method to statistical testing in deformation analysis based on robust M-estimation. Survey Review, 48, No. 346, 212–223. DOI: 10.1179/1752270615Y.0000000026

Nowel, K. and Kamiński, W.: 2014, Robust estimation of deformation from observation differences for free control networks. Journal of Geodesy, 88, No. 8, 749–764. DOI: 10.1007/s00190-014-0719-7

Pelzer, H.: 1971, Zur Analyse geodetischer Deformation-smessung. DGK, Reihe C, Heft N 164, Munchen.

Pope, J.: 1976, The statistics of residuals and detection of outliers. NOAA Technical Report Nos. 66 NGS 1.

Prószyński, W.: 2010, Another approach to reliability measures for systems with correlated observations. Journal of Geodesy, 84, No. 9, 547–556. DOI: 10.1007/s00190-010-0394-2

Setan, H. and Singh, R.: 2001, Deformation analysis of a geodetic monitoring network. Geomatica, 55, No. 3, 333–346.

Sušić, Z., Batilović, M., Ninkov, T., Aleksić, I. and Bulatović, V.: 2015, Identification of movements using different methods of deformation analysis. Geodetski vestnik, 59, No. 3, 537–553. DOI: 10.15292/geodetski-vestnik.2015.03.537-553

Sušić, Z., Toljić, M., Bulatović, V., Ninkov, T. and Stojadinović, U.: 2016, Present-day horizontal mobility in the Serbian part of the Pannonian Basin, inferences from the geometric analysis of the deformations. Acta Geophysica, 64, No. 5, 1629–1654. DOI: 10.1515/acgeo-2016-0074

Talich, M.: 2007, Geometrical analysis of deformation measurement using continuum mechanics by Web application. FIG Working Week, Hong Kong SAR, China, 13-17 May.

Toljić, M., Matenco, L., Ducea, M.N., Stojadinović, U., Milivojević, J. and Đerić, N.: 2013, The evolution of a key segment in the Europe–Adria collision: The Fruška Gora of northern Serbia. Global and Planetary Change, 103, 39–62. DOI: 10.1016/j.gloplacha.2012.10.009, 2013

Velsink, H.: 1983, On the deformation analysis of point fields. Journal of Geodesy, 89, No. 11, 1071–1087. DOI: 10.1007/s00190-015-0835-z

Welsch, W.: 1983, Finite element analysis of strain patterns from geodetic observations across a plate margin. Tectonophysics, 97, No. 1, 57–71. DOI: 10.1016/0040-1951(83)90125-7

Wiśniewski, Z.: 2009, Estimation of parameters in a split functional model of geodetic observations (Msplit estimation). Journal of Geodesy, 83, No. 2, 105–120. DOI: 10.1007/s00190-008-0241-x

Xu, P.L.: 2005, Sign-constrained robust least squares, subjective break down point and the effect of weights of observations on robustness. Journal of Geodesy, 79, No. 1-3, 146–159. DOI: 10.1007/s00190-005-0454-1

Zienkiewicz, M.H. and Baryla, R.: 2015, Determination of vertical indicators of ground deformation in the Old and main city of Gdansk area by applying unconventional method of robust estimation. Acta Geodynamica et Geomaterialia, 12, No. 3(179), 249–257. DOI: 10.13168/AGG.2015.0024

Zienkiewicz, M.H.: 2014, Application of Msplit estimation to determine control points displacements in networks with an unstable reference system. Survey Review, 47, No. 342, 174–180. DOI: 10.1179/1752270614Y.0000000105

Zienkiewicz, M.H., Hejbudzka, K. and Dumalski, A.: 2017, Multi split functional model of geodetic observations in deformation analyses of the Olsztyn Castle. Acta Geodyn. Geomater., 14, No. 2 (186), 195–204. DOI: 10.13168/AGG.2017.0003

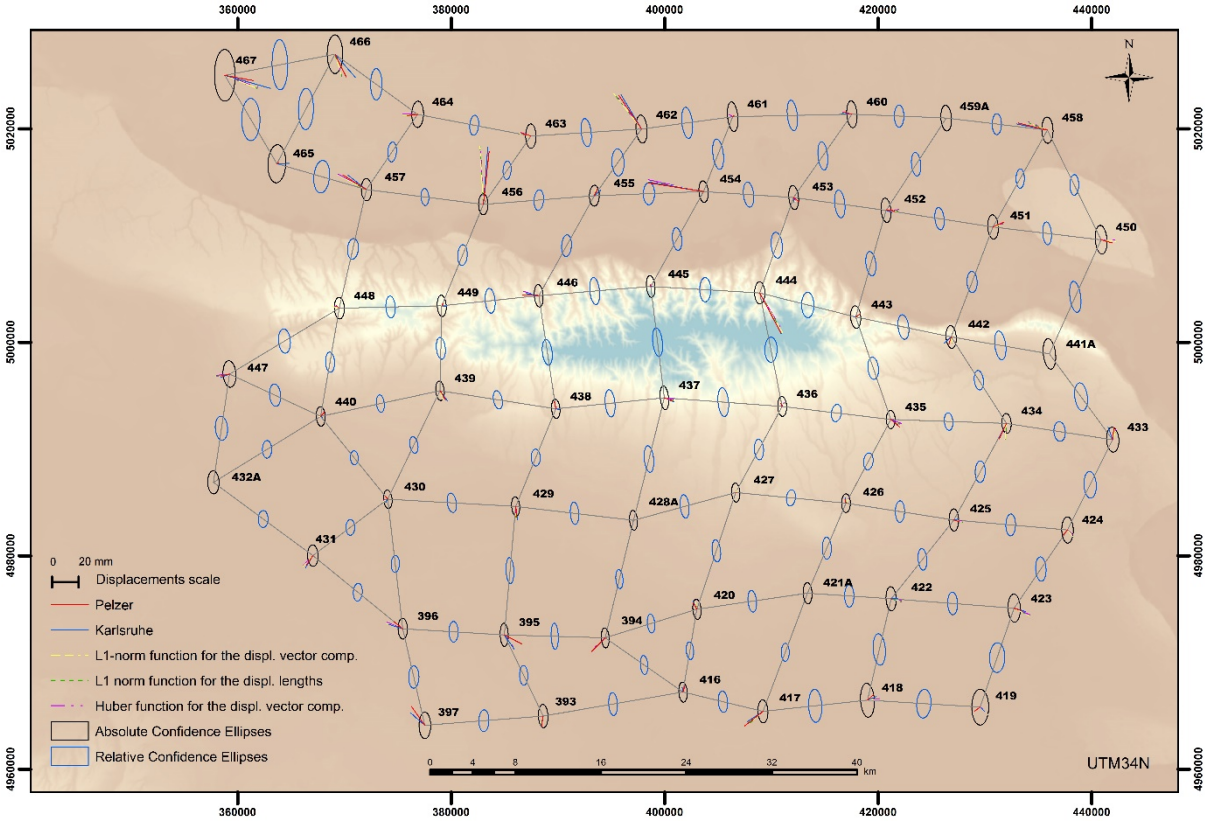

Fig. 2 Displacement vectors of the CDA and robust methods applied in the work (shown in the DEM of the Fruška Gora area).

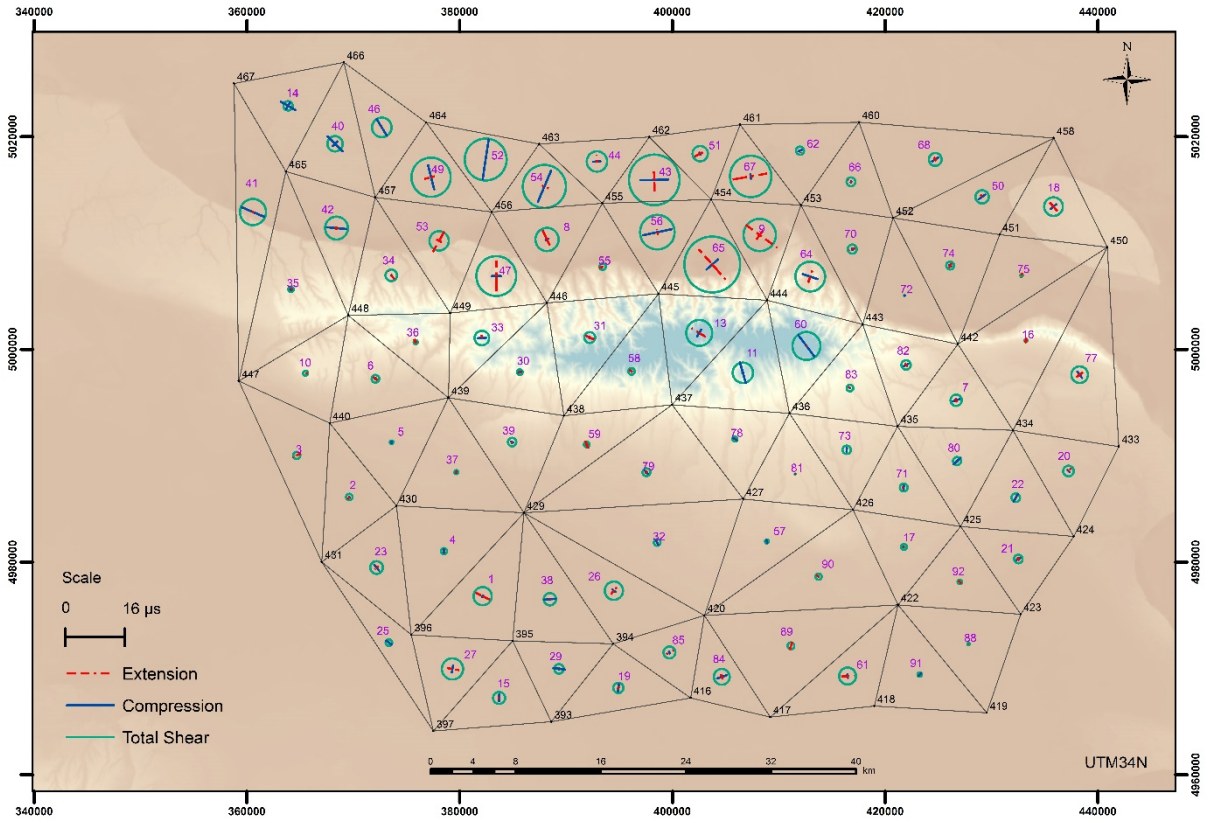

Fig. 3 Principal strain parameters computed for each triangle in the network (shown in the DEM of the Fruška Gora area).